Since January 2020 Elsevier has created a COVID-19 resource centre with free information in English and Mandarin on the novel coronavirus COVID-19. The COVID-19 resource centre is hosted on Elsevier Connect, the company's public news and information website.

Journal of Drug Delivery Science and Technology 79 (2023) 104082

Contents lists available at ScienceDirect

Journal of Drug Delivery Science and Technology

journal homepage: www.elsevier.com/locate/jddst

Development of favipiravir loaded PLGA nanoparticles entrapped in in-situ gel for treatment of Covid-19 via nasal route

Vaishnavi Gattani [a], Shilpa Dawre [a,b,*]

[a] Department of Pharmaceutics, School of Pharmacy & Technology Management, SVKMS, NMIMS, Babulde Banks of Tapi River, MPTP Park, Mumbai-Agra Road, Shirpur, Maharashtra, 425405, India
[b] Department of Pharmaceutics, School of Pharmacy, Vishwakarma University, Laxmi Nagar, Kondhwa, Pune, Maharashtra, 411048, India

ARTICLE INFO

Keywords:
Favipiravir
Mucoadhesion
PLGA Nanoparticles
Thermoreversible in-situ gel
Nasal *ex vivo* permeation
Box-behnken design

ABSTRACT

In 2019 the emergence of SARS-COV-2 caused pandemic situation worldwide and claimed ~6.4 M lives (WHO 2022). Favipiravir (FAV) is recommended as a therapy for Covid-19 which belongs to BCS class III with a short half-life of 2–5.5h. Thus, the objective of current study was the development of favipiravir loaded PLGA nanoparticles (NPs) by box-behnken design. Moreover, these NPs were entrapped in thermosensitive gel to increase the permeation through nasal route. The nanoparticles exhibit particle size of 175.6 ± 2 nm with >70 ± 0.5 % EE. NPs showed PDI (0.130) and zeta potential (−17.1 mV) suggesting homogeneity and stability of NPs. DSC, XRD, and FTIR studies concluded absence of any interaction of FAV and the excipients. SEM and AFM studies demonstrated spherical morphology of NPs with smooth surface. The NPs entrapped in-situ gel showed clarity and pH 5.5–6.1. The gelation temperature of NPs dispersed in-situ gel was found in the range of 35 °C −37 °C. The gel has viscosity in range of 34592–4568 cps. The texture analysis profile of gel showed good gelling properties. Dissolution study suggested a sustained release of FAV from NPs (24h) and NPs dispersed gel (32h) as compared to FAV solution (4h). The gel showed good mucoadhesion properties (9373.9 dyne/cm^2). *Ex-vivo* permeation through nasal mucosa of goat elucidated NPs dispersed gel demonstrated significantly higher permeation than solution and NPs. Therefore, it would be a prospective formulation to combat Covid-19 infection with high patient compliance.

1. Introduction

The severe acute respiratory syndrome coronavirus-2 (SARS COV-2) is a new-fangled microorganism and origin of Covid-19 pandemic situation globally [1]. Current therapies, research & development groups, and medical facilities of all countries were trying to find solutions and therapies of the Covid-19 infection that has claimed ~6.4 M lives to date [2]. This viral strain is extremely infectious and contagious. It causes flu-like symptoms causing severe respiratory syndrome leading to death due to respiratory failure [3]. Many antivirals were repurposed that could be useful against this unique coronavirus, due to the lack of new drugs to combat the condition. In addition, the occurrence of multidrug resistance and low antiviral concentration at the site of infection posed challenges in treatment [4]. Thus, there is a need of new formulation strategies and modalities that could assist in tackling this Covid-19 infection.

Numerous novel formulations such as solid lipid nanoparticles [5,6], liposomes, NLCs [7], nanoparticles (NPs), etc. have been studied for delivery of drugs via nasal route. Moreover, these novel formulations were explored as a therapy of Covid-19 infection [8] and amongst these nanoparticles were successfully applied for development of vaccine [9]. PLGA is a U.S. FDA approved biodegradable polymer with great efficiency of drug loading. It has been previously explored for development of nanoparticles loaded with variety of drugs. Surnar B. et al. developed ivermectin encapsulated nanoparticles using PLGA polymer modified with PEG and maleimide (PLGA-*b*-PEG-Mal). Furthermore, they had decorated nanoparticles by Fc immunoglobulin fragment to cross the epithelial layer of gut which allowed drug to reach into bloodstream. *In vitro* cytotoxicity and uptake studies in HEK293T cells showed better uptake of NPs than free drug. Moreover, oral bioavailability of drug was found higher than drug solution [10]. Ucar et al. designed oseltamivir-phosphate loaded PLGA nanoparticles decorated by means peptide binder of SARS-COV-2 spike protein for ACE-2 receptor

* Corresponding author. Department of Pharmaceutics, School of Pharmacy & Technology Management, SVKMS, NMIMS, Babulde Banks of Tapi River, MPTP Park, Mumbai-Agra Road, Shirpur, Maharashtra, 425405, India.
E-mail addresses: shilpadawre@vupune.ac.in, shilpa.dawre@vupune.ac.in (S. Dawre).

https://doi.org/10.1016/j.jddst.2022.104082
Received 7 October 2022; Received in revised form 8 December 2022; Accepted 10 December 2022
Available online 13 December 2022

Abbreviations

FAV	Favipiravir
SARS-COV-2	Severe-acute respiratory syndrome corona virus-2
DOE	Design of Experimentation
PLGA	Poly-Latic-Glycolic acid
HPMC	Hydroxy-Propyl Methyl Cellulose
BBD	Box-Behnken, design
%EE	% Entrapment Efficiency
PDI	Poly dispersity index
FTIR	Fourier Transforms Infrared spectroscopy
DSC	Differential-Scanning-Calorimetry
SEM	Scanning Electron Microscopy
AFM	Atomic force microscopy
XRD	X-ray diffraction
PBS	Phosphate Buffer Saline
NPs	Nanoparticles
ANOVA	Analysis of variance

targeting. Nanoparticles demonstrated a sustained release of drug for two months [11]. In another study Wu et al. developed lisinopril tagged nanoparticles loaded with remdesivir by molecular docking approach to target on angiotensin-converting enzyme −1 receptor [12].

Favipiravir (FAV) is a molecule approved in Japan for treatment of influenza virus infection and recently approved as a therapy of SARS-COV-2. It specifically inhibits viral RNA-dependent RNA polymerase (RdRp). Earlier studies revealed that favipiravir showed antiviral activity for large range of RNA viruses than other antiviral agents [13]. The available marketed formulation of favipiravir is oral tablet (Avigan®, Fabiflu®). The dosing frequency of FabiFlu® is 18 tablets on day 1 (200 mg) (nine in the morning and nine in the evening), trailed by eight tablets each day subsequently for a maximum of 14 days. It is highly patient incompliance with high toxicity and adverse effects [14]. Furthermore, FAV belongs to the BCS class III with a short half-life of 2–5.5h. Therefore, to decrease this dose size and dosing frequency, there is a need of novel formulation. The intranasal route could be suitable route for Covid-19 treatment that can deliver high drug concentration at the target site and circumvent undesirable adverse effects as lower doses are required [15]. Moreover, it avoids first pass metabolism and related side effects. Gilead Sciences, USA also conducting clinical trials of remdesivir in inhaled form for Covid-19 [16].

In the present study we have prepared and optimized FAV loaded PLGA nanoparticles (NPs) by using box-behkhen design for sustained release action. Furthermore, these nanoparticles were entrapped in thermosensitive in situ-gel for enhancement of nasal permeation. The developed formulation showed sol to gel transition gel in nasal area which could reduce mucociliary clearance and can allow NPs to diffuse through nasal mucosa. Moreover, intranasal route enhances patient compliance and reduce dose & dosing frequency. FAV-NPs and FAV-NPs dispersed in-situ gel were assessed for physicochemical characteristics, dissolution pattern, and permeation through nasal mucosa of goat.

2. Materials and methods

2.1. Materials

Favipiravir was generously presented by Viruj Pharmaceuticals (Hyderabad, India). The polymer Poly lactide-*co*-glycolide (PLGA, 50:50) was donated by Evonik India Pvt. Ltd. (Mumbai, India). Other polymers Hydroxy-Propyl Methyl Cellulose (HPMC) and Kolliphor P-407 & Kolliphor P-188 were bought from Rankem Labs, Mumbai, India and BASF, India, respectively. Other chemicals like hydrogen chloride, sodium hydroxide, potassium dihydrogen orthophosphate phosphate, acetonitrile, acetone, and analytical grades solvents were procured from SD Fine Chem, (India).

2.2. Methods

2.2.1. Development of FAV nanoparticles

The nanoprecipitation method was used to prepare nanoparticles with little modification [17]. The organic phase was produced by solubilizing PLGA (5 mg & 20 mg) and favipiravir (30 mg & 200 mg) in acetone (10 mL). Poloxamer 407 (10 mg & 20 mg) was solubilized in water (20 mL) to make an aqueous phase. After that it was placed on water bath for complete dissolution and cooled for 10–15 min. Then an aqueous phase was mixed gradually into an organic phase. The acetone was then permitted to evaporate for 3h by stirring emulsion via magnetic stirrer. Later nanoparticles were centrifuged at 14,000 rpm for 20 min. The nanoparticles were collected and rinsed three times with distilled water.

2.2.2. Nanoparticles optimization by design of experimentation

Optimization of the favipiravir loaded polymeric nanoparticles was done with box-behnken design (BBD) using three parameters at two levels. The selected optimization parameters were favipiravir concentration (X1), the PLGA amount (X2), and Poloxamer 407 amount (X3) were considered as an independent parameter and the two dependent factors, particles size (Y1) and percentage entrapment efficiency (Y2) were considered (Table 1). Table 2 illustrates trials suggested by software with five center locations. To elude biasness, the trials were conducted randomly.

The DOE generated the non-linear quadratic design, which was found to be

$$Y = b0 + b1X1 + b2X2 + b3X3 + b4X1X2 + b5X1X3 + b6X2X3 + b7\,X21 + b8X22 + b9X23$$

In the above equation Y represents the response due to the interaction of all factors in combination. The intercept is b0, and the regression coefficients are b1-b9, were obtained from the experimental outcomes. The independent factors are X1, X2, and X3. The additional parameters (mixing time, non-aqueous and aqueous phase amount, etc.) were retained constant. The statistical data from the linear regression as well as the 3D surface response graphs were examined using Design-Expert® Version 11.

2.2.3. Development of FAV-NPs entrapped gel

The in-situ gel was developed by using previously reported cold method [18]. Poloxamer 407 (2 gm) and Poloxamer 188 (0.5 gm) were accurately weighed and added slowly in nanoparticle suspension at 4 °C

Table 1
Independent parameters for design of nanoparticles by BBD.

No.	Parameters	Low (mg)	High (mg)
1	FAV amount	30	200
2	PLGA amount	5	20
3	Poloxamer 407 amount	10	20

Table 2
Outcome of independent parameters on response factors.

Run	Parameter 1	Parameter 2	Parameter 3	Response 1	Response 2
	X1: Favipiravir amount	X2: PLGA amount	X3: Poloxamer amount	Y1: Particle size	Y2: Entrapment efficiency
	mg	Mg	mg	nm	%
1	115	20	15	208.2	73.72
2	**115**	**11.5**	**10**	**175.6**	**78.24**
3	115	11.5	10	175.6	78.24
4	200	11.5	5	180.5	74.23
5	115	3	5	171.5	69.63
6	30	20	10	196.1	65.59
7	115	20	5	179.9	72.35
8	30	11.5	15	168.9	68.89
9	200	11.5	15	188.8	72.56
10	115	11.5	10	175.6	78.24
11	200	20	10	212.24	75.54
12	115	3	15	148.8	65.23
13	200	3	10	168.8	68.23
14	30	11.5	5	188.5	67.35
15	30	3	10	174.5	62.54
16	115	11.5	10	175.6	78.24
17	115	11.5	10	175.6	78.24

temperature. The blend was agitated using a magnetic stirrer at 800 rpm (Remi Lab, India) till polymers were solubilized. After that hydroxyl propyl methyl cellulose (1% w/v) solution which is a mucoadhesive polymer was mixed and solubilized in above mixture. The developed gel was characterized for gel properties.

2.2.4. Evaluation of FAV nanoparticles

2.2.4.1. Entrapment-efficiency (%EE). The amount of favipiravir encapsulated in nanoparticle was determined by using UV spectroscopy. Nanoparticles dispersion was rotated at 14000 rpm at 4 °C for 20mins by using centrifuge. After this the supernatant was accumulated and diluted with ethanol. Then analyzed for FAV by UV spectrophotometer at ƛmax 237 nm. The formula; % EE = quantity of FAV in nanoparticles/theoretical amount of drug * 100 was utilized. In which the theoretical amount signifies the amount of drug initially loaded in NPs.

2.2.4.2. ζ-potential, polydispersity index, & particle size. The size of FAV NPs was calculated by utilizing dynamic light scattering technology (Malvern particle size analyser 2000 series, UK). The nanoparticle dispersion (0.5 mL) was prepared in purified water (10 mL) using ultrasonic homogenizer (DP120, Mumbai, India) operated at 150 voltages with on-off cycle of 10s for 5mins. The particle size analysis was conducted at scattering angle of 90° at 25 °C. Then this dispersion was analyzed for ζ-potential, polydispersity index, and particle size.

2.2.4.3. FTIR study. FTIR scanning of FAV, Poloxamer-407, PLGA, and excipients with FAV was carried out by using Shimadzu Affinity- 1S. All the samples were in powder from, small quantity of this sample was carefully kept into the empty space and later were examined at resolution of 4/cm $^{-1}$ in the IR area (400–4000/cm $^{-1}$).

2.2.4.4. DSC study. Favipiravir, PLGA, and FAV-loaded nanoparticles were analyzed for DSC at warming rate of 10 °C (DSC 60 Shimadzu). Samples were analyzed at 30 °C – 400 °C. The movement of heat is from the primary and secondary warming gradients used to determine the melting temperature (Tm).

2.2.4.5. XRD study. X-ray diffraction study was done by using Philips Analytical Xperto Pro PW-1710, with a resolution of 0.001A. The diffraction pattern of samples was recorded with 2 θ range of 5–60° in the steps of 0.01o/sec. Cu Kα radiation operated at 40 kV and 30 mA was used as an X-ray source.

2.2.4.6. Scanning electron microscopy (SEM). The superficial structure of nanoparticles was studied by scanning electron microscope (ZEISS, SUPRA 55VP). The nanoparticle suspension was fixed upon a slide (1*1 cm) using a tape. Then sputtered with gold and observed using microscope at a magnifying power of 13830. Polymeric nanoparticles shape and size were recorded.

2.2.4.7. Atomic force microscopy (AFM). Atomic force microscopy was assessed utilizing dimension XR. The nanoparticles were diluted with distilled water and dried on mica coated glass slide. The images were taken with a silicon-type probe in non-contact operating mode [19]. Then the slide was analyzed under 100 μ m scanner and canteliver of 25 N/m and of radius 10 nm.

2.2.4.8. Stability studies. The stability NPs was checked in accordance with International Council of Harmonization guidelines Q1(R2). The nanoparticles were placed for six months at 70 ± 5% RH and 40 ± 2 °C. The aliquots were taken and assessed for their %EE, particle size, and physical appearance in every one month.

2.2.5. Evaluation of FAV-NPs entrapped gel

2.2.5.1. Transparency and pH. The gel was cautiously inspected under brightened background for any sign of foreign particles or turbidity. The pH of the gel was calculated by an electronic pH meter (LABINDIA Pico^{+} design).

2.2.5.2. Viscosity measurement. The viscosity of gel was performed utilizing 10 ml of gel in beaker under Brookfield digital DV-II Model. The viscous property of gel was tested at different speed (10–100). The generated % torque was recorded.

2.2.5.3. Gelation temperature. The temperature at which gel formation occurs was determined by stirring 20 ml gel at 37 °C and speed of 50 rpm. The degree centigrade condition at which the magnetic bar become steady was recorded.

2.2.5.4. Texture profile. The gel texture profile was assessed using an instrument (TA-XT texture analyser). The gel (10 mL) was kept in a beaker and adjusted under analyser at 25 mm height at 37 ± 2 °C. After that a probe was permitted to insert at least 10 mm inside the gel at a speed of 2 mm/s. Then the probe was raised slowly which allows the detachment of gel from the layer. The power requisite for separation provides the gel strength.

2.2.6. Dissolution studies

The dissolution profile of favipiravir was conducted using Franz diffusion cell [20]. The FAV release pattern was assessed form solution, FAV-NPs, and FAV-NPs distributed gel. The dissolution media used was Phosphate Buffer (PBS) at 5.5 pH. The cellophane membrane (capacity

2.41 mL/cm and diameter 17.5 mm) was measured as per requirement and activated in PBS 5.5. After 24h the cellophane membrane was washed with purified water to eradicate any impurity, then placed in Franz diffusion cell apparatus. Weighed quantity of FAV solution, FAV-NPs dispersion, and FAV-NPs dispersed gel were taken in equivalence to the drug concentration (3 ml = 17 mg) and kept into donor cell. The receptor cell was filled with dissolution media (20 ml). The apparatus was then placed at 37 °C onto a stirrer (300 rpm). The sample of 1 ml was withdrawn at various time points (30mins, 1, 1.5, 2, 2.5, 3, 4, 6, 8, 12, 24, 28, & 32h) and was replenished with PBS for each aliquot. The aliquots were evaluated by the UV spectrophotometer for FAV at 237 nm.

2.2.7. Mucoadhesion study

The nasal mucosal adhesion of the FAV-NPs dispersed gel was performed by finding out the power needed to remove formulation adhered to mucosal sheath. The nasal mucosa of goat was procured from a local butcher shop and adhere on to the vial (0.785 cm^2 surface area). The upper probe attached with the mucosal sheath by using cyanoacrylate adhesive. However, gel was attached with the bottom side of probe and allowed to maintained at 37 °C. Force of 0.1 N was utilized to assure close contact between the mucosa and gel. An equilibrium tool was utilized for the upward movement of upper and lower probes at a constant rate (0.15 nm/s). The formula, mucoadhesive strength = Fmax *g/A was applied for calculation of mucoadhesive strength of gel in dyne/cm^2. Wherein, F_{max} = maximum force required for separation (grams), g = acceleration due to gravity [980 cm/s^2], and A = area of mucosa layer attached.

2.2.8. Ex vivo permeation study

The permeation of FAV solution, FAV-NPs, and FAV-NPs dispersed gel were conducted using nasal mucosa of goat [19]. It was obtained from local slaughter shop. Then mucosa was placed in Franz diffusion cell (area 2.0 cm^2 & thickness of 0.3 mm). Two minutes were spent after adhering the nasal mucosa so that the drug solution or gel should not get leaked. The FAV suspension in phosphate buffer, FAV-NPs dispersion, and FAV-NPs dispersed gel 100 μL (1.4 mg/ml) were placed separately in different cells. The samples were taken at interval of 5, 15, 30 min, 1h, 2h, 4h, & 6h which was replaced by fresh phosphate buffer at every point of collection of samples. The aliquots were examined for FAV by validated RP-HPLC method at 237 nm. Aliquots were individually substituted by an equivalent amount media. The graph was plotted between cumulative amount of FAV permeated from nasal mucosa *vs* time to calculate flux. The below mentioned formula was utilized to calculate permeability coefficient (P):

$$P = dQ/dt\ CoA$$

where Co indicates the initial concentration in the donor cell, dQ/dt signifies the rate of permeability or flux [mg/h], and A epitomizes the active area of the nasal mucosa.

2.2.9. Statistical study

The standard deviation and mean were calculated for entire data set. Dunnett's test and one-way ANOVA on data was conducted by GraphPad Prism 5, USA software, in which $p < 0.05$ indicates a considerable difference.

Table 4
Resultant p-values of dependent factors.

Variables	p-value of NPs particle size	p-value of %EE
X1	0.0108	<0.0001
X2	<0.0001	<0.0001
X3	0.4093	0.2007
X1X2	0.0021	0.0310
X1X3	0.0005	0.0820
X2X3	<0.0001	0.0082
$X1^2$	0.0001	<0.0001
$X2^2$	0.0106	<0.0001
$X3^2$	0.0722	0.0003

3. Results and discussion

3.1. Development of nanoparticles

Favipiravir encapsulated polymeric nanoparticles were successfully prepared using nanoprecipitation technique with high drug loading (>70%). Nanoprecipitation technique provide nanoparticles with high encapsulation efficiency [21]. Furthermore, these NPs were successfully entrapped in thermosensitive in-situ gel for enhancement of nasal permeation.

3.2. Nanoparticles optimization by design of experimentation

The BBD design was utilized for development of NPs. The impact of independent factors (X1) such as FAV amount, (X2) PLGA amount, and (X3) Poloxamer 407 amount on responses (NPs size and %EE) studied by response surface methodology (RSM). The software suggested 17 runs with 5-center points and formulations were designed (Table 2). Moreover, software provided quadratic equation that explains the interaction of all variables and their effects. The significance level (5%) of the quadratic equations was measured by ANOVA. Tables 3 and 4 illustrates the coefficients of quadratic equation and p-values. The desirability value of optimized formulation was found 0.85 which is close to an ideal value 1. The desirability value equal to 0 was considered not satisfactory, however a value near to 1 signified an acceptable value [22].

3.2.1. Influence on particle size

The following equation illustrates the influence of several independent variables on the particle size (Y1):

$$\text{Particle size}(y) = 175.60 + 2.79x_1 + 16.61x_2 - 0.7125x_3 + 5.46x_1x_2 + 6.98x_1x_3 + 12.75x_2x_3 + 8.44x_1^2 + 3.87x_2^2 - 2.37x_3^2$$

The F-value of the model was 76.41, concluded that the design was significant ($p < 0.001$). The correlation between the experimental and estimated values was indicated by the R^2 of 0.9899. The "Predicted R^2" (0.8388) and "Adjusted R^2" of 0.9770, suggested that the design was found to be accurate to predict the outcomes. The S/N ratio was used to compute "adequate precision." The resultant ratio of 10.94 recommended that the signal was within acceptable range. A percent CV of 1.27 reflected the model's precision and reliability.

The p-value was utilized to predict the effects of coefficients. The lower the p-value, the greater the significance of the associated coefficient. The model terms are significant when "Prob > F" (<0.05). Table 4 elucidates that the all-design variables X1, X2, X3, X1X2, X2X3, and

Table 3
Summarization of model properties for responses Y1 and Y2.

Models	R^2	Adjusted R^2	Predicted R^2	SD	Adequate precision	% CV	Remarks
Particle size (Y1)							
Quadratic	0.9899	0.9770	0.8388	2.30	37.31	1.27	Significant
% Entrapment efficiency (Y2)							
Quadratic	0.9901	0.9774	0.8417	0.79	25.004	1.10	Significant

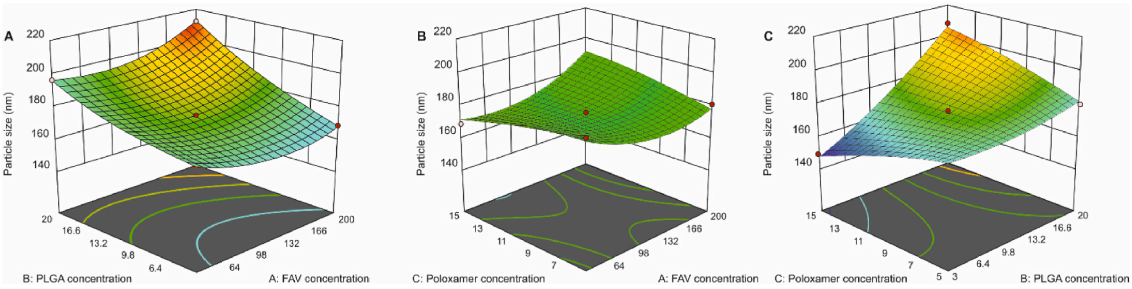

Fig. 1. 3D surface Plots of A) showing effects of PLGA concentration (X2) and Favipiravir Concentration (X1); B) showing effects of Poloxamer 407 concentration (X3) and Favipiravir Concentration (X1) C) PLGA concentration (X2) and Poloxamer concentration (X3) on response particle size (Y1).

X1X3 were significant. A positive symbol signifies a synergistic effect; however, negative symbol denotes an antagonistic result.

The RSM plot illustrates the influence of independent parameters on nanoparticles size (Fig. 1). It was detected that with increase in the PLGA amount, there was increase in NPs size occurred. This effect was observed due to increase in polymer concentration that resulted into enhancement in viscosity and created problem in preparation of minute globules at steady mixing speed [23]. Thus, high particle size was obtained owing to high concentration of PLGA. These results were in accordance with study done by Huang et al. They had studied effect of varied PLGA concentrations on particle size and concluded that concentration of PLGA is directly proportional with the NPs size [24].

Additionally, the concentration of surfactant is an important risk analysis parameter in development of nanoparticles and it is a primary influencer on nanoparticle size [25]. Generally, it has been observed that concentration of poloxamer 407 is inversely proportional with the nanoparticle size. The surfactant plays a crucial role in reduction of surface tension and provide stability to nanoparticles [26]. In our study it was observed that enhancement of the poloxamer 407 concentration reduces NPs size, however, after some point, increase in particle size was observed. The probable reason could be as initially the amount of poloxamer 407 could be sufficient for reduction of particle size. Nevertheless, further increase in surfactant concentration caused increase in particle size due to adsorption of poloxamer 407 on NPs surface resulted formation of thick coating [27]. Furthermore, with increase in surfactant amount viscosity of aqueous phase also rises resulting large particle size [28].

The above-mentioned results were in accordance with previous studies [27,29,30]. Sakhi and co-authors developed polymeric nanoparticles loaded with paclitaxel for treatment of breast cancer. They observed similar results as with increase in poloxamer concentration PLGA, NPs size increases [27]. Thus, it could be concluded that concentrations of polymer and surfactant both significantly effect NPs size.

3.2.2. Influence on %EE

The polynomial equation obtained for %EE is mentioned below:

$$(y2) = 78.26 + 5.70x_1 - 0.7900x_2 + 1.25x_3 + 3.05x_1x_2 + 0.7500x_1x_3 - 2.37x_2x_3 - 6.40x_1^2 - 4.54x_2^2 - 2.31x_3^2$$

The F-value 77.81 illustrates the model is significant ($p < 0.0001$). The coefficient of regression (R^2) of the design was obtained 0.9901. The "Predicted R^2", "Adjusted R^2" (0.8417, 0.9774), and percent CV (1.10%) confirmed good model fit.

The results indicate that as the concentration of PLGA increases there is rise in %EE, however, after a definite point there was reduction in % EE occurred (Fig. 2). This might be due to increase in viscosity of the phases with increase in PLGA amount, attributed rapid solidification and

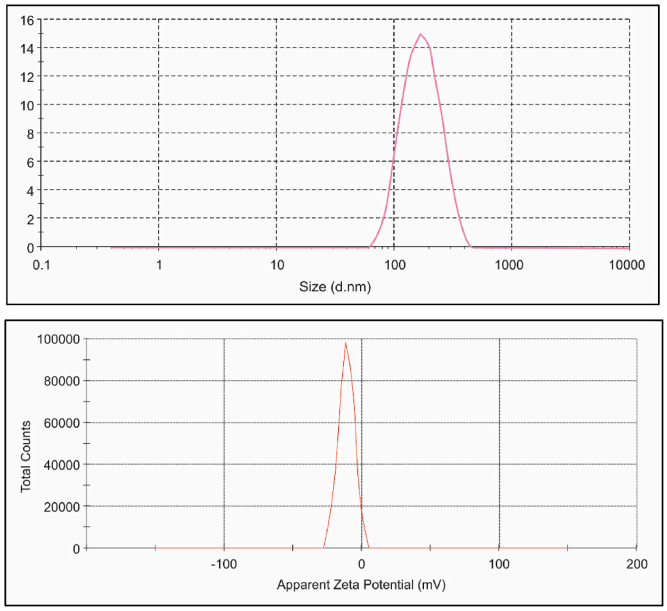

Fig. 3. Particle size distribution and ζ-potential of FAV NPs.

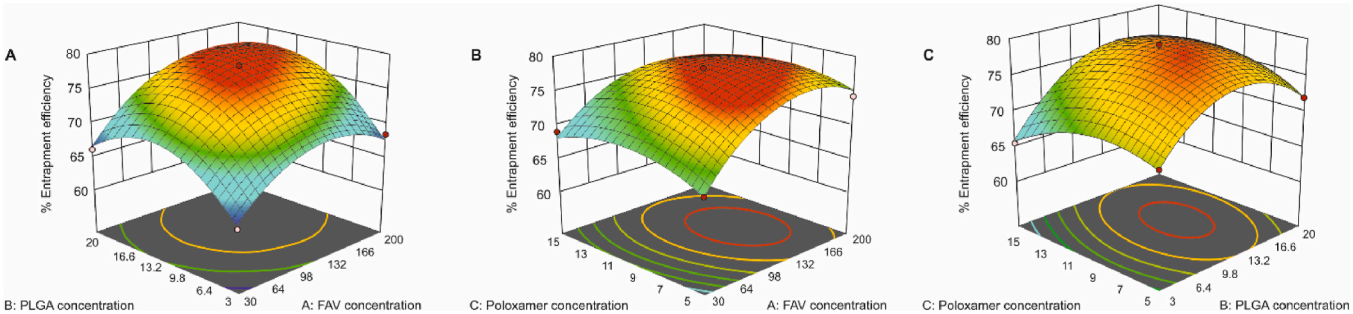

Fig. 2. 3D surface plots of A) showing effects of Favipiravir concentration (X1) and PLGA concentration (X2); B) Favipiravir concentration (X1) and Poloxamer concentration (X3) C) PLGA concentration and Poloxamer concentration response entrapment efficiency (Y2).

slower diffusion of drug from interior to exterior region [24]. On the other hand, as the concentration of surfactant Poloxamer 407 increased the dispersal of drug in both aqueous and non-aqueous phases occurred. Furthermore, surfactant also enhanced drug solubility in exterior phase and improves stability of the w/o emulsion [31]. Thus, decrease in %EE was observed with increase in poloxamer 407 concentration.

3.3. Evaluation of FAV-nanoparticles

3.3.1. Entrapment efficiency

Entrapment efficiency is an important criterion in preparing the favipiravir loaded polymeric nanoparticles, as well as it has been proved to be an important variable in the optimization of nanoparticles. To obtain precise drug encapsulation, the factors such as PLGA concentration and Poloxamer 407 concentration were found to be important factors. The optimized formula of nanoparticles (Formula 2) has %EE >70%.

3.3.2. ζ-potential, polydispersity index, & particle size

The nanoparticles revealed size distribution in range of 175.6 ± 3 nm with PDI 0.130 suggesting that the particle size was evenly distributed throughout the dispersion and have a uniform size (Fig. 3). Zeta potential helps in understanding stability of NPs. Zeta potential values higher than +30 mV and less than −30mV, considered as stable [32]. However, it was observed that PLGA NPs mostly carries negative charge due to presence of carboxyl group [33]. Thus, the zeta potential of FAV-NPs was observed −17.5mv due to the charge on the PLGA molecule. Cui et al. also reported stable PLGA nanoparticles loaded with doxorubicin and paclitaxel which showed zeta potential in the range of −9.0mv to −18.0 mv [34].

3.3.3. Scanning electron microscopy

SEM study demonstrated that FAV-NPs exhibit spherical morphology and possessed a smooth surface which in agreement with dynamic light scattering analysis (Fig. 4). The image illustrates absence of aggregation or crysallization of drug molecule and confirmed uniformity of nanoparticles. Moreover, spherical morphology with smooth surface could result into sluggish clearance and good deposition pattern in nasal area. The results were in accordance with prior study by Patil et al. They reported that ropinirole hydrochloride encapsulated PLGA NPs for nasal delivery and revealed that cicular NPs diffuses slowly through nasal mucosa as compared to rod-shaped NPs [35].

3.3.4. FTIR analysis

FTIR transforms of FAV, PLGA, Poloxamer, and overlay plot shown in Fig. 5 (A, B, C, D). Favipiravir transform of FAV revealed all typical peaks such as band developed due to vibrations & stretching of carbonyl bond (C═O) at 1716 cm^{-1}, ether (C–*O*–C) band at 1180 cm^{-1} and vibrations stretching of amine N–H at 3347 cm^{-1} & 3212 cm^{-1} [36]. The transform of poloxamer 407 showed band of esters (C–*O*–C) at 1240 cm^{-1}, vibrations stretching of (O–H at 3647.2 cm^{-1} & amine bond (N–H) at 3347 cm^{-1}). The FTIR of PLGA suggests presence of a band of vibrations stretching of CH2 at 2294.7 cm^{-1}, band of cyclic alcohols (C–OH) at 1087 cm^{-1}, and vibrations stretching of carbonyl (C═O) at 1716 cm^{-1} [37]. Nevertheless, the overlay transforms of FAV with excipients demonstrated all primary peaks of FAV such as band developed due to vibrations & stretching of carbonyl bond (C═O) at 1716 cm^{-1}, ether (C–*O*–C) band at 1180 cm^{-1} and vibrations stretching of amine N–H at 3347 cm^{-1} & 3212 cm^{-1}. Thus, FTIR study confirmed absence of interaction between favipiravir and the excipients demonstrating compatibility during formulation development.

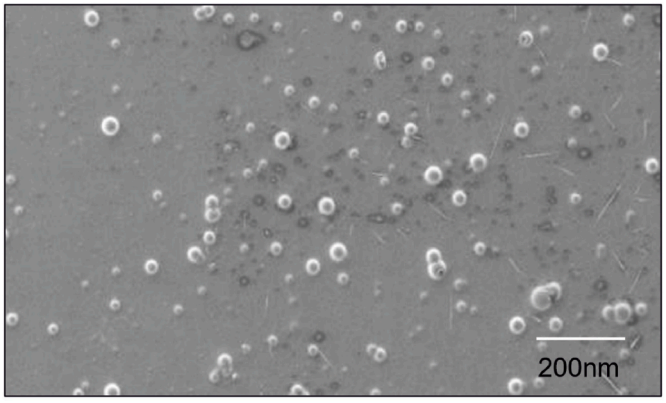

Fig. 4. SEM image of FAV nanoparticles.

3.3.5. DSC study

DSC thermometry result of PLGA and FAV represented in Fig. 6. DSC study demonstrated that FAV showed the presence of endotherms at 189.91 °C, implying crystallinity. The melting endotherms of favipiravir has not been observed in nanoparticles, indicating amorphous form [38]. Additionally, DSC study also suggested formation of nanoparticles with encapsulation of drug inside nanoparticles.

3.3.6. Atomic force microscopy (AFM)

The structure of FAV NPs was evaluated by AFM (Fig. 7). The nanoparticle exhibits spherical morphology which is in corroboration with SEM studies. Additionally, the AFM technique showed that the size of the NPs was lesser than that detected by the DLS system. The possible reason could be due to the procedural differences in measurement of size. Singh et al. mentioned that the DLS method assess the hydrodynamic particle size, which was observed every time bigger than the real size [39]. Kurtosis measures the sharpness of the peak [40]. When the skewness value ranges in 0.5–1 then it is considered skewed. If the value lies in ranges of −0.5 to 0.5 specifies symmetrical distribution. The skewness and kurtosis values were found to be 0.966 and 6.49, respectively which showed that the values are in acceptable range.

3.3.7. XRD study

X-ray diffractogram is the fingerprint region which was observed due to peculiar crystalline structures of compounds. Fig. 8 illustrates X-ray diffractogram of FAV and FAV-NPs. The characteristics sharp and intense peak of favipiravir was obsereved by XRD. Whereas, the XRD diffractograms of nanoparticles showed less intensity of FAV suggesting amporphization of drug which is in coroborration with DSC studies [38].

3.3.8. Stability studies

The preparations were examined for appearance, particle size, and % entrapment efficiency. At the, end of, six months' nanoparticles were found to be at stable at 40 °C and 75% RH. Table 5 represents the stability studies of NPs with their % entrapment efficiency and particle size. The stability studies confirmed that NPs were found stable over six months indicating good stability.

3.4. Evaluation of FAV-NPs entrapped gel

3.4.1. Transparency and pH

The nasal gel was found transparent and had no additional particles. Gel showed clarity, good texture, and pH (5.5–6.1) suggesting suitability for delivery by nasal route.

3.4.2. Gelation temperature

The nasal area has temperature ranging 35–37 °C. The sol initiated to convert into gel at 37 °C, suggesting that gel has appropriate gelation temperature required for administration via nasal route. The combination of poloxamer polymers was responsible for formation of transparent gel. It was observed that as the Poloxamer 407 amount rise, the gelation-temperature slowly decreases. However, if the Poloxamer 188

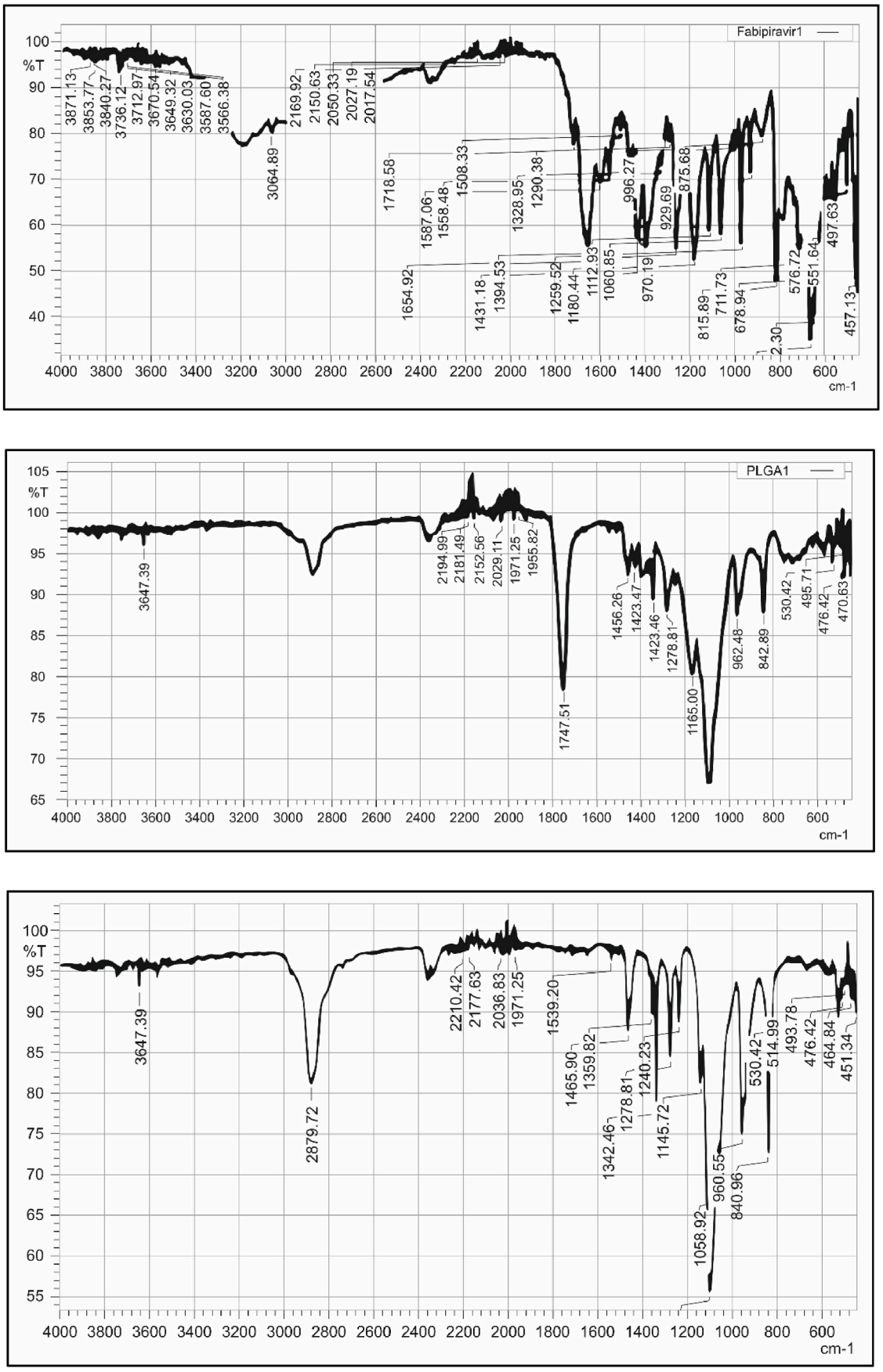

Fig. 5. FTIR transforms of A) Favipiravir B) PLGA C) Poloxamer D) Favipiravir and excipient E) Over lay plot.

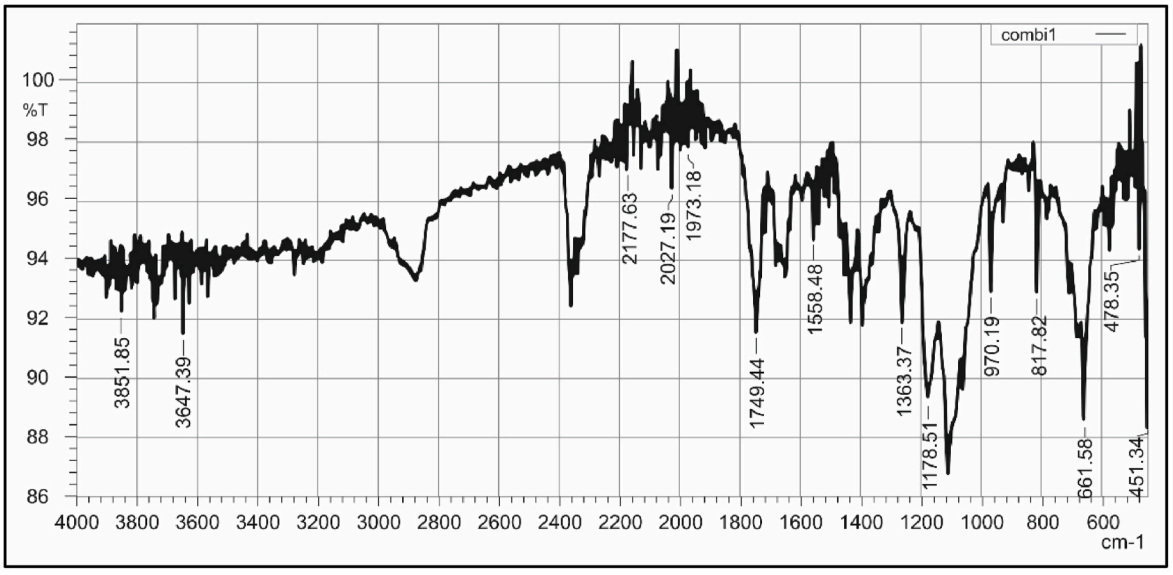

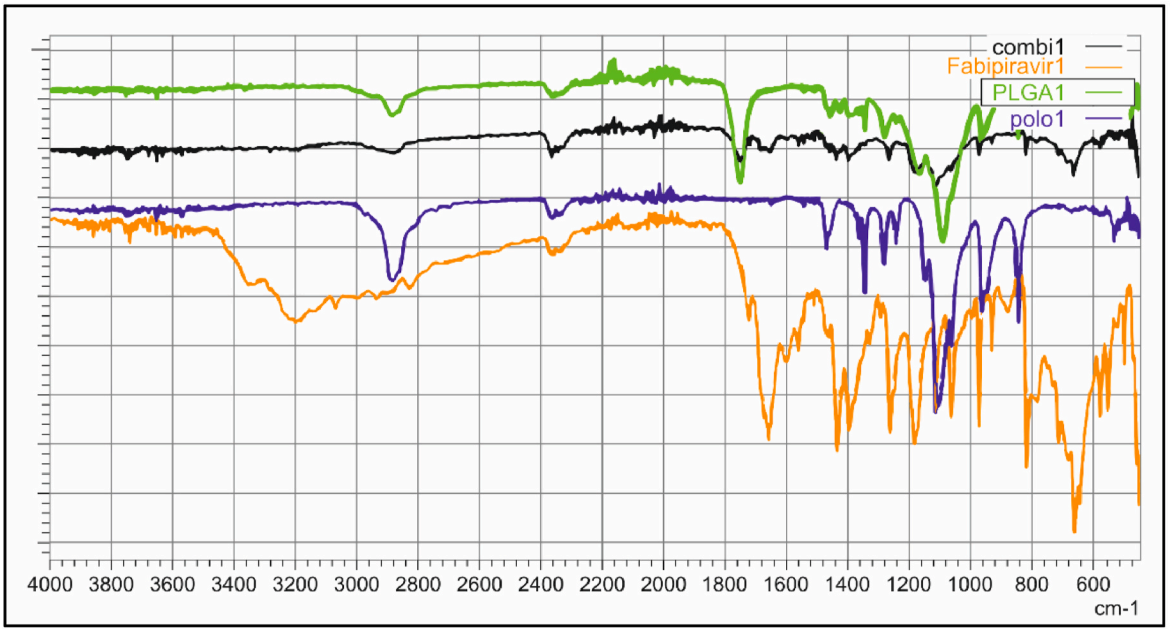

Fig. 5. (*continued*).

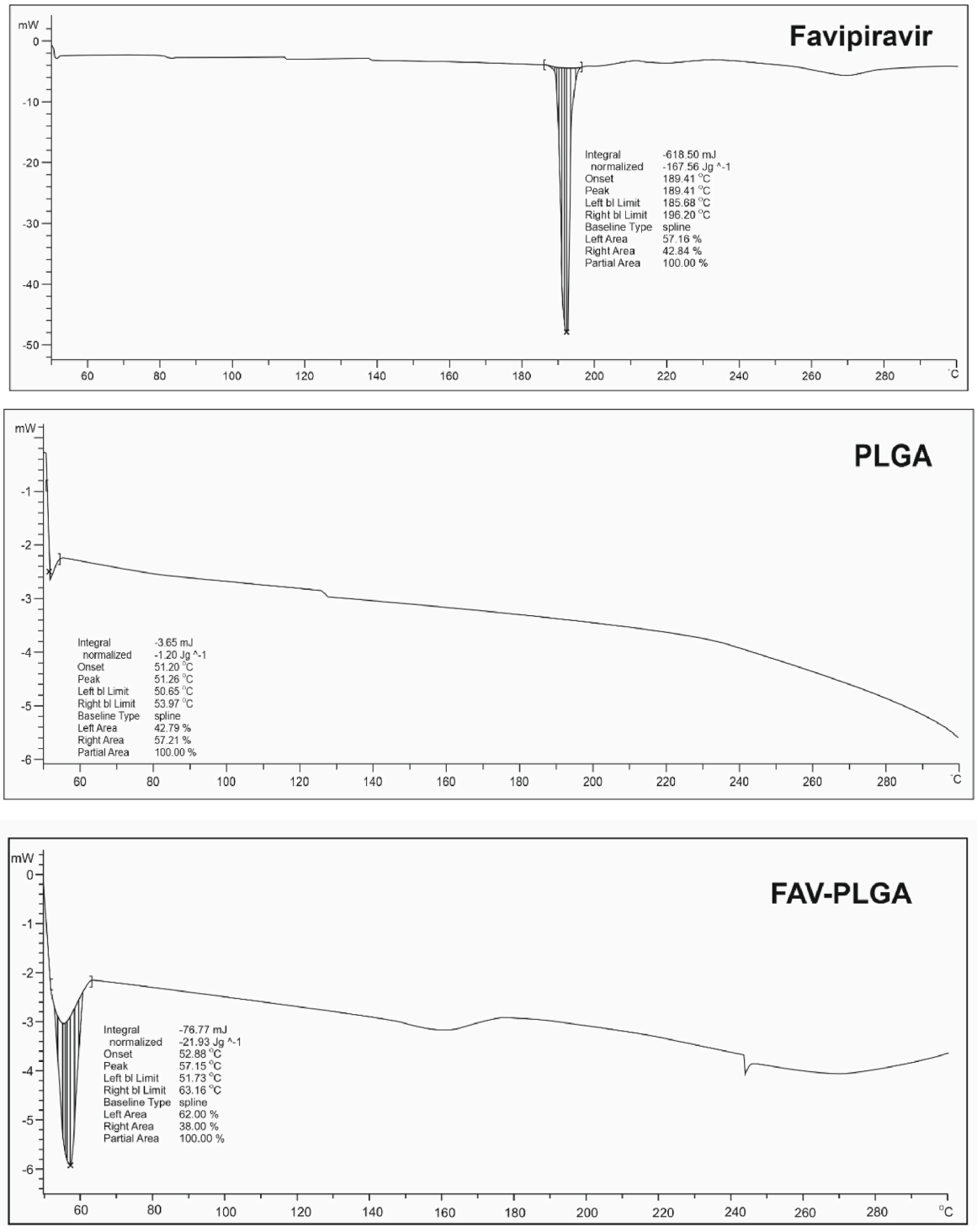

Fig. 6. DSC thermogram of a) Favipiravir (b) PLGA (c) Favipiravir-PLGA NPs.

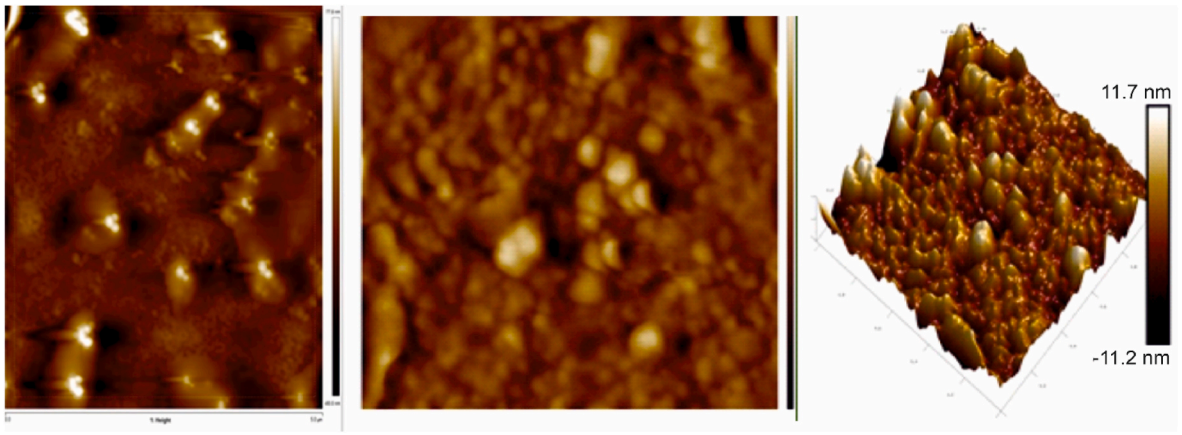

Fig. 7. AFM studies of favipiravir nanoparticles.

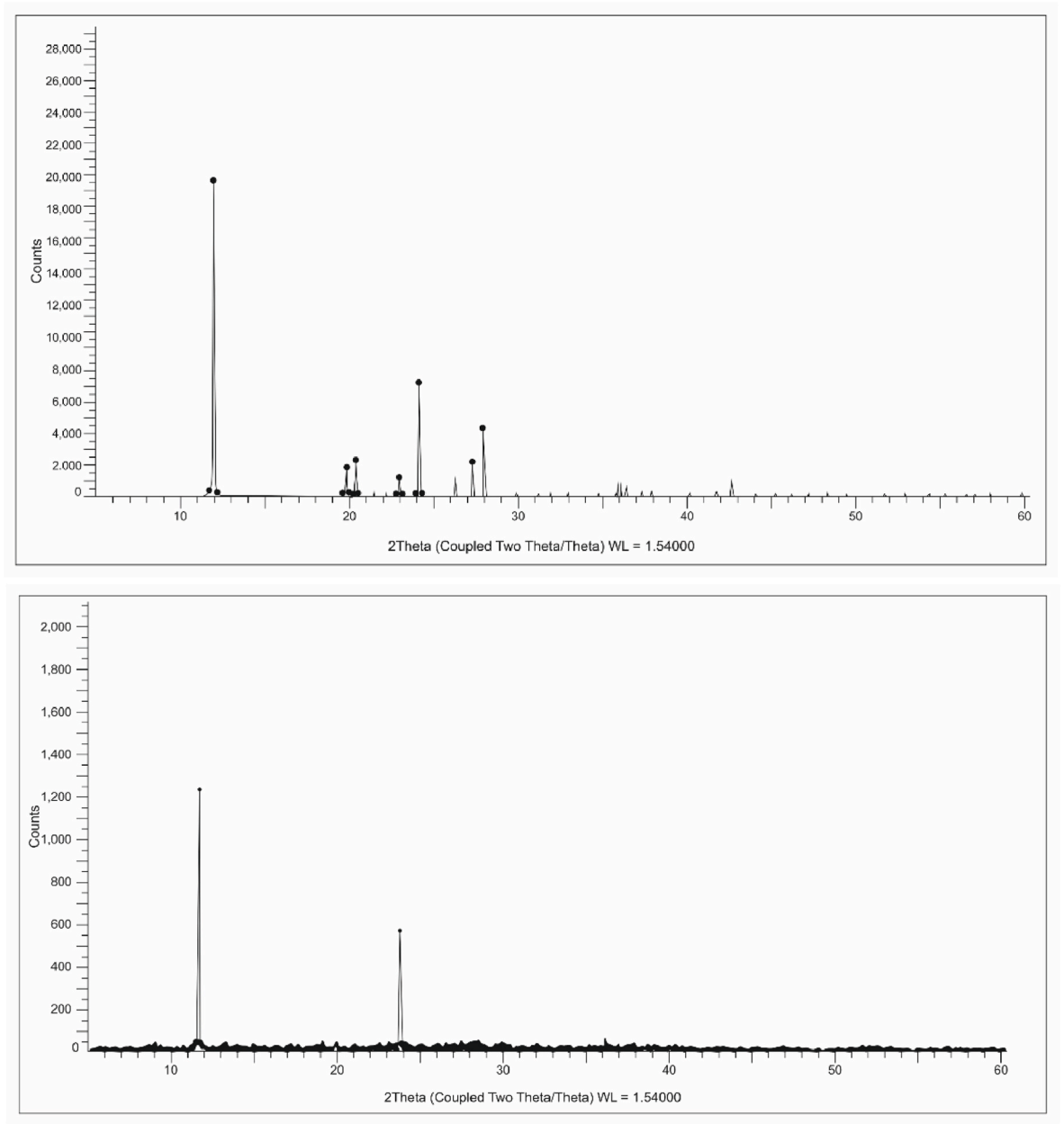

Fig. 8. XRD graph of a) Favipiravir and b) Favipiravir loaded nanoparticles.

Table 5
Accelerated stability studies.

Months	% Entrapment efficiency	Particle size (nm)
Initial	78.12 ± 0.15%	175±1 nm
1	78.12 ± 0.25%	176±2 nm
2	77.92 ± 0.1%	179±1 nm
3	76.50 ± 0.3%	179±1 nm
4	75.12 ± 0.1%	180±1 nm
5	75.11 ± 0.11%	181±1 nm
6	75.00 ± 0.15%	182±2 nm

concentration enhanced, the temperature was also increased. Thus, Poloxamer 407 and 188 were incorporated combinely, to control the gelation temperature that provided appropriate mucoadhesion and gelation [18].

3.4.3. Viscosity measurement

The gel viscosity was observed in range of 34592–4568 cps with the torque lies in range of 62–85.5% from 10 to 100 rpm. It was observed that HPMC, poloxamer 407, and poloxamer 188 concentrations contributed in maintaining the gel viscosity. The formation of 3D matrix occurred due to crosslinking of polymers which helps in maintaining the viscosity of gel. Poloxamers and HPMC usually contains hydrogen bonds and electrostatic interactions which aids in viscosity maintenance and mucoadhesion properties [41].

3.4.4. Texture profile

The texture profiling is an imperative property in development of nasal gel. The texture analysis of thermoreversible gel was shown in Fig. 9 and elucidated hardness at 16 g, adhesiveness of 1.01 mJ, gumminess of 14 g, cohesiveness of 2.34, and stringiness of 1.46 mm at 37 °C. Hardness and adhesiveness helps in finding out ease in application and detachment of gel from the surface. The gel strength of the gel was found 1.2 ± 0.3 mJ suggesting good strength. Gel strength is explained as capacity of sol to convert into intact gel [42]. The HPMC and poloxamers combinely contributed in providing strength to gel and adhesive property. Gel strength evidenced that the gel is firm, thus, it could resist the nasal mucociliary clearance.

3.4.5. Mucoadhesion study

Mucoadhesion strength helps to evaluate the strength and the impact of polymers over the biological surface, the mucoadhesion is the amount of adhesion on mucosal surface that the polymer can show (by binding onto the mucosal surface), at a bodily temperature. In this experiment the contact time of the polymer to the nasal membrane with respect to time was measured. If the contact time decreases, then the mucoadhesion strength of the polymer is also less [43]. The mucoadhesion of the thermoreversible gel was found out to be 9373.9 dyne/cm^2 indicating good adhesion on mucosa. Therefore, in the nasal cavity, the NPs dispersed gel can hold for an elongated period resulting increase in permeation and FAV absorption.

3.4.6. Dissolution studies

Sample and separate technique was utilized to find out release pattern of FAV from formulations. The study revealed that favipiravir solution showed 90% drug release in 4h. However, nanoparticles showed a sustained release of favipiravir for more than 20h. The NPs dispersed gel showed 79% of FAV release up to 32h (Fig. 10). Nanoparticles revealed a prolonged release of FAV because of polymeric matrix. The entrapment of FAV inside PLGA matrices decelerated release rate that could be controlled by diffusion and erosion of polymer membrane. These results were in agreement with prior studies [44,45]. Nevertheless, FAV-NPs dispersed gel showed more prolonged release than polymeric nanoparticles due to the presence of dual barrier of swelled hydrogel phase and polymer [44,46].

The release kinetics of preparations were calculated by release models. Table 6 exemplified calculated coefficient of correlation (R^2). The FAV solution demonstrated First order release pattern (R^2 = 0.9704). Nonetheless, release data of nanoparticles and nanoparticles distributed in gel fitted well in Koresmeyer-Peppa's model (R^2 = 0.9771, 0.9578). It suggests that the favipiravir discharge by dual mechanism from NPs i.e. slow diffusion through PLGA mesh and destruction of nanoparticles [47].

3.4.7. Ex vivo permeation study

Permeation study across nasal mucosa of goat suggested higher permeation of FAV nanoparticles distributed in gel as compared to nanoparticles dispersion and drug solution ($P < 0.05$) (Fig. 11). It was indicated by the permeability coefficient (P), flux enhancement ratio, and steady-state flux (fss) (Table 7).

The NPs dispersed gel displayed 4.5 times greater permeation than solution and 1.8 times than nanoparticles. The significantly high *ex vivo* penetration of FAV-NPs distributed gel through the nasal mucosa might

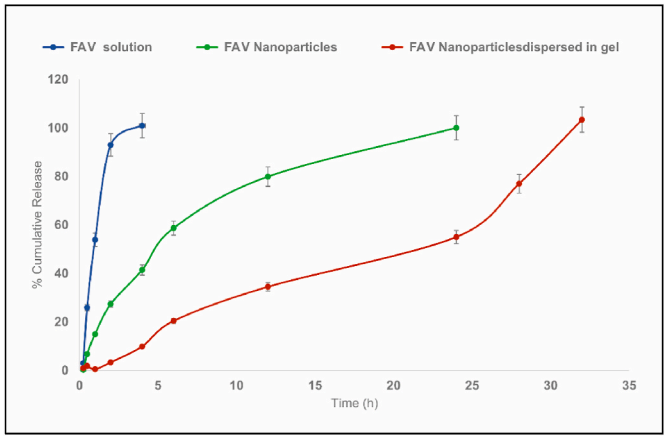

Fig. 10. Dissolution study of Favipiravir solution, nanoparticles and nanoparticles dispersed gel.

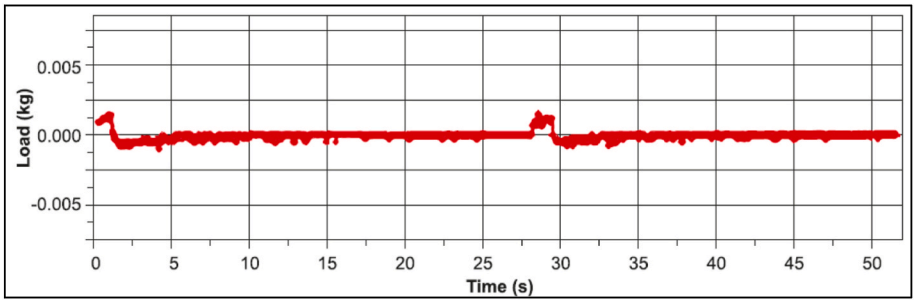

Fig. 9. Texture profiling of thermoreversible gel.

Table 6
Drug release kinetics.

Description	R^2 Value			
	Zero Order	First Order	Higuchi Plot	Korsmeyer-Peppa Plot
Favipiravir solution	0.8554	**0.9704**	0.8979	0.9473
Favipiravir nanoparticles	0.9669	0.7606	0.9647	**0.9771**
Favipiravir nanoparticles dispersed in Gel	0.9472	0.9089	0.8923	**0.9578**

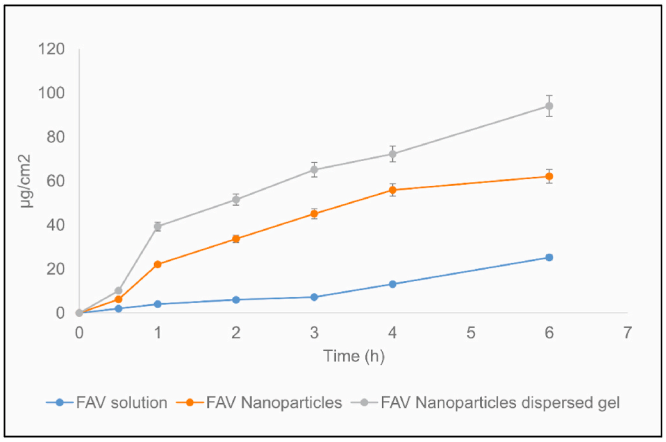

Fig. 11. *Ex vivo* permeation studies of favipiravir from solution, nanoparticles, and nanoparticles loaded gel.

be due to the adherence of NPs dispersed gel on the mucosal sheath which resulted high permeation rate. Moreover, mucoadhesive polymer HPMC also contributed in elongated interaction time of formulation and nasal mucosal surface resulting improved permeation of FAV [48]. However, solution and nanoparticles have no mucoadhesion and high fluidity. Thus, contact time with mucosal layer is less resulting small permeability of FAV. Literature confirmed that improvement of contact time statistical enhance drug permeation [49]. These results were in agreement with a previous study in which NLC dispersed gel displayed better permeation (1.5 folds) than drug solution [50].

4. Conclusion

The stable nanoparticles with good entrapment efficiency (>70%) and particle size (175.6 nm) were successfully optimized by using box-behkhen design. Nanoparticles demonstrated spherical morphology and smooth surface. In-vitro release study showed a sustained release property of NPs (20h). Nanoparticles dispersed thermoreversible in-situ gel was developed which showed good texture analysis profile. Additionally, gel showed good mucoadhesive properties supporting nasal permeation. The NPs dispersed gel showed prolonged release for more than 30h. *Ex vivo* permeation through goat's nasal mucosa confirmed that NPs dispersed gel demonstrated higher permeation of FAV than NPs and solution. Therefore, FAV nanoparticles in-situ gel could be a promising treatment for Covid-19 infection via nasal route. This formulation could reduce high dose and dosing frequency of oral FAV and could be a new patient friendly alternative therapy for Covid-19. Nevertheless, *in vivo* studies are required to understand the efficacy of formulation.

Table 7
Ex vivo permeation study of formulations.

	FAV solution	FAV Nanoparticles	FAV Nanoparticles entrapped gel
Flux ss (µg. $Cm^{-2}.h^{-1}$)	2.011 ± 0.16	5.01 ± 0.31	9.41 ± 0.93
Enhancement ratio	–	3.08 ± 0.31	4.6 ± 0.5
Permeability coefficient (cm/h)	0.00287	0.0071	0.01344

Consent for publication

I give my consent to publish this research article in this journal.

Funding for publication

Not applicable.

CRedit author statement

Conceptualization: Dr. Shilpa Dawre.
Methodology: Dr. Shilpa Dawre and Vaishnavi Gattani.
Validation: Dr. Shilpa Dawre.
Investigation: Vaishnavi Gattani.
Data Curation: Dr. Shilpa Dawre and Vaishnavi Gattani.
Writing: Dr. Shilpa Dawre and Vaishnavi Gattani.
Supervision: Dr. Shilpa Dawre.

Declaration of competing interest

The authors declare that they have no conflict of interest.

Data availability

Data will be made available on request.

Acknowledgements

Authors want to acknowledge R.C Patel institute Shirpur for the XRD analysis.

References

[1] S. Dawre, S. Maru, Human respiratory viral infections: current status and future prospects of nanotechnology-based approaches for prophylaxis and treatment, Life Sci [Internet] 278 (2021 Aug), 119561. Available from: https://linkinghub.elsevier.com/retrieve/pii/S0024320521005476.
[2] Worldometer [Internet], Available from: https://www.worldometers.info/coronavirus/.
[3] B. Hu, H. Guo, P. Zhou, Z.-L. Shi, Characteristics of SARS-CoV-2 and COVID-19, Nat. Rev. Microbiol. [Internet] 19 (3) (2021 Mar 6) 141, 54. Available from: https://www.nature.com/articles/s41579-020-00459-7.
[4] R.K. Guy, R.S. DiPaola, F. Romanelli, R.E. Dutch, Rapid repurposing of drugs for COVID-19, May 22, Science (80-) [Internet] 368 (6493) (2020) 829, 30. Available from, https://www.science.org/doi/10.1126/science.abb9332.
[5] M. Yasir, U.V.S. Sara, I. Chauhan, P.K. Gaur, A.P. Singh, D. Puri, et al., Solid lipid nanoparticles for nose to brain delivery of donepezil: formulation, optimization by Box–Behnken design, in vitro and in vivo evaluation. Artif Cells, Nanomedicine, Biotechnol [Internet] (2017 Nov 3) 1–14. Available from: https://www.tandfonline.com/doi/full/10.1080/21691401.2017.1394872.
[6] M. Yasir, I. Chauhan, A. Zafar, M. Verma, K.M. Noorulla, A.J. Tura, et al., Buspirone loaded solid lipid nanoparticles for amplification of nose to brain efficacy: formulation development, optimization by Box-Behnken design, in-vitro characterization and in-vivo biological evaluation, J. Drug Deliv. Sci. Technol. [Internet] 61 (2021 Feb), 102164. Available from: https://linkinghub.elsevier.com/retrieve/pii/S1773224720314532.
[7] M. Yasir, A. Zafar, K.M. Noorulla, A.J. Tura, U.V.S. Sara, D. Panjwani, et al., Nose to brain delivery of donepezil through surface modified NLCs: formulation development, optimization, and brain targeting study, J. Drug Deliv. Sci. Technol. [Internet] 75 (2022 Sep), 103631. Available from: https://linkinghub.elsevier.com/retrieve/pii/S1773224722005421.
[8] M. Abd Elkodous, S.O. Olojede, M. Morsi, G.S. El-Sayyad, Nanomaterial-based drug delivery systems as promising carriers for patients with COVID-19, RSC Adv. [Internet 11 (43) (2021) 26463–26480. Available from: http://xlink.rsc.org/?DOI=D1RA04835J.
[9] L. Schoenmaker, D. Witzigmann, J.A. Kulkarni, R. Verbeke, G. Kersten, W. Jiskoot, et al., mRNA-lipid nanoparticle COVID-19 vaccines: structure and stability, Int. J. Pharm. [Internet] 601 (2021 May), 120586. Available from: https://linkinghub.elsevier.com/retrieve/pii/S0378517321003914.

[10] B. Surnar, M.Z. Kamran, A.S. Shah, S. Dhar, Clinically approved antiviral drug in an orally administrable nanoparticle for COVID-19, ACS Pharmacol. Transl. Sci. [Internet 3 (6) (2020 Dec 11) 1371, 80. Available from: https://pubs.acs.org/doi/10.1021/acsptsci.0c00179.

[11] B. Ucar, T. Acar, P.P. Arayici, S. Derman, A nanotechnological approach in the current therapy of COVID-19: model drug oseltamivir-phosphate loaded PLGA nanoparticles targeted with spike protein binder peptide of SARS-CoV-2, Nanotechnology [Internet] 32 (48) (2021 Nov 26), 485601. Available from: https://iopscience.iop.org/article/10.1088/1361-6528/ac1c22.

[12] J. Wu, H. Wang, B. Li, Structure-aided ACEI-capped remdesivir-loaded novel PLGA nanoparticles: toward a computational simulation design for anti-SARS-CoV-2 therapy, Phys. Chem. Chem. Phys. [Internet 22 (48) (2020), 28434, 9. Available from: http://xlink.rsc.org/?DOI=D0CP04389C.

[13] S. Joshi, J. Parkar, A. Ansari, A. Vora, D. Talwar, M. Tiwaskar, et al., Role of favipiravir in the treatment of COVID-19, Int. J. Infect. Dis. [Internet] 102 (2021 Jan) 501–508. Available from: https://linkinghub.elsevier.com/retrieve/pii/S1201971220322736.

[14] U. Agrawal, R. Raju, Z.F. Udwadia, Favipiravir: a new and emerging antiviral option in COVID-19, Med. J. Armed Forces India [Internet] 76 (4) (2020 Oct) 370–376. Available from: https://linkinghub.elsevier.com/retrieve/pii/S0377123720301581.

[15] T. Saha, M.E. Quiñones-Mateu, S.C. Das, Inhaled therapy for COVID-19: considerations of drugs, formulations and devices, Int. J. Pharm. [Internet] 624 (2022 Aug), 122042. Available from: https://linkinghub.elsevier.com/retrieve/pii/S037851732200597X.

[16] clinical trials [Internet]. Available from: https://clinicaltrials.gov/ct2/show/NCT04539262.

[17] Y. Herdiana, N. Wathoni, S. Shamsuddin, M. Muchtaridi, Scale-up polymeric-based nanoparticles drug delivery systems: development and challenges, OpenNano [Internet] 7 (2022 Jul), 100048. Available from: https://linkinghub.elsevier.com/retrieve/pii/S2352952022000111.

[18] [Internet] Y. Wang, S. Jiang, H. Wang, H. Bie, A mucoadhesive, thermoreversible in situ nasal gel of geniposide for neurodegenerative diseases, 12(12), in: B. Xu (Ed.), PLoS One, 2017 Dec 14, e0189478. Available from: https://dx.plos.org/10.1371/journal.pone.0189478.

[19] M. Giannouli, V. Karagkiozaki, F. Pappa, I. Moutsios, C. Gravalidis, S. Logothetidis, Fabrication of quercetin-loaded PLGA nanoparticles via electrohydrodynamic atomization for cardiovascular disease, 6005, Mater. Today Proc. [Internet 5 (8) (2018), 15998. Available from: https://linkinghub.elsevier.com/retrieve/pii/S2214785318309155.

[20] M. Ochi, B. Wan, Q. Bao, D.J. Burgess, Influence of PLGA molecular weight distribution on leuprolide release from microspheres, Int. J. Pharm. [Internet] 599 (2021 Apr), 120450. Available from: https://linkinghub.elsevier.com/retrieve/pii/S0378517321002556.

[21] M. Chorny, I. Fishbein, H.D. Danenberg, G. Golomb, Lipophilic drug loaded nanospheres prepared by nanoprecipitation: effect of formulation variables on size, drug recovery and release kinetics, J. Control Release [Internet] 83 (3) (2002 Oct) 389–400. Available from: https://linkinghub.elsevier.com/retrieve/pii/S0168365902002110.

[22] M. Haider, A. Elsherbeny, J. Jagal, A. Hubatová-Vacková, I. Saad Ahmed, Optimization and evaluation of poly(lactide-co-glycolide) nanoparticles for enhanced cellular uptake and efficacy of paclitaxel in the treatment of head and neck cancer, Pharmaceutics [Internet] 12 (9) (2020 Aug 30) 828. Available from: https://www.mdpi.com/1999-4923/12/9/828.

[23] K. Jokicevic, S. Kiekens, E. Byl, I. De Boeck, E. Cauwenberghs, S. Lebeer, et al., Probiotic nasal spray development by spray drying, Eur. J. Pharm. Biopharm. [Internet] 159 (2021 Feb) 211–220. Available from: https://linkinghub.elsevier.com/retrieve/pii/S0939641120303416.

[24] W. Huang, C. Zhang, Tuning the size of poly(lactic-co-glycolic acid) (PLGA) nanoparticles fabricated by nanoprecipitation, Biotechnol. J. [Internet] 13 (1) (2018 Jan), 1700203. Available from: https://onlinelibrary.wiley.com/doi/10.1002/biot.201700203.

[25] H. Cortés, H. Hernández-Parra, S.A. Bernal-Chávez, ML Del Prado-Audelo, I. H. Caballero-Florán, F.V. Borbolla-Jiménez, et al., Non-ionic surfactants for stabilization of polymeric nanoparticles for biomedical uses, Materials (Basel) [Internet] 14 (12) (2021 Jun 10) 3197. Available from: https://www.mdpi.com/1996-1944/14/12/3197.

[26] D. Sharma, D. Maheshwari, G. Philip, R. Rana, S. Bhatia, M. Singh, et al., Formulation and optimization of polymeric nanoparticles for intranasal delivery of lorazepam using box-behnken design: in vitro and in vivo evaluation, Biomed. Res. Int. [Internet] 2014 (2014) 1–14. Available from: http://www.hindawi.com/journals/bmri/2014/156010/.

[27] M. Sakhi, A. Khan, Z. Iqbal, I. Khan, A. Raza, A. Ullah, et al., Design and characterization of paclitaxel-loaded polymeric nanoparticles decorated with Trastuzumab for the effective treatment of breast cancer, Front. Pharmacol. [Internet] (2022). Mar 14;13, 1-15. Available from: https://www.frontiersin.org/articles/10.3389/fphar.2022.855294/full.

[28] R. Pradhan, B.K. Poudel, T. Ramasamy, H.-G. Choi, C.S. Yong, J.O. Kim, Docetaxel-loaded polylactic acid-Co-glycolic acid nanoparticles: formulation, physicochemical characterization and cytotoxicity studies, J Nanosci Nanotechnol [Internet 13 (8) (2013 Aug 1) 5948–5956. Available from: http://openurl.ingenta.com/content/xref?genre=article&issn=1533-4880&volume=13&issue=8&spage=5948.

[29] C. Draheim, F. de Crécy, S. Hansen, E.-M. Collnot, C.-M. Lehr, A design of experiment study of nanoprecipitation and nano spray drying as processes to prepare PLGA nano- and microparticles with defined sizes and size distributions, Pharm. Res.2015, 2(8), 2609-24 [Internet] (2015 Feb 13). Available from: http://link.springer.com/10.1007/s11095-015-1647-9.

[30] E. Snejdrova, J. Loskot, J. Martiska, T. Soukup, L. Prokes, V. Frolov, et al., Rifampicin-loaded PLGA nanoparticles for local treatment of musculoskeletal infections: formulation and characterization, J. Drug Deliv. Sci. Technol. [Internet] 73 (2022 Jul), 103435. Available from: https://linkinghub.elsevier.com/retrieve/pii/S1773224722003458.

[31] P. Girotra, S.K. Singh, G. Kumar, Development of zolmitriptan loaded PLGA/poloxamer nanoparticles for migraine using quality by design approach, Int J Biol Macromol [Internet] 85 (2016 Apr) 92–101. Available from: https://linkinghub.elsevier.com/retrieve/pii/S0141813015302567.

[32] J.D. Clogston, A.K. Patri, Zeta Potential Measurement, 2011, pp. 63–70. Available from: http://link.springer.com/10.1007/978-1-60327-198-1_6.

[33] H.I. Chiu, N.A. Samad, L. Fang, V. Lim, Cytotoxicity of targeted PLGA nanoparticles: a systematic review, RSC Adv. [Internet 11 (16) (2021) 9433–9449. Available from: http://xlink.rsc.org/?DOI=D1RA00074H.

[34] Y. Cui, Q. Xu, P.K.-H. Chow, D. Wang, C.-H. Wang, Transferrin-conjugated magnetic silica PLGA nanoparticles loaded with doxorubicin and paclitaxel for brain glioma treatment, Biomaterials [Internet] 34 (33) (2013 Nov) 8511–8520. Available from: https://linkinghub.elsevier.com/retrieve/pii/S0142961213008892.

[35] G.B. Patil, S.J. Surana, Fabrication and statistical optimization of surface engineered PLGA nanoparticles for naso-brain delivery of ropinirole hydrochloride: in-vitro–ex-vivo studies [Internet], J. Biomater. Sci. Polym. 24 (15) (2013 Oct 24) 1740, 56. Available from, https://www.tandfonline.com/doi/full/10.1080/09205063.2013.798880.

[36] A.S. Tulbah, W.-H. Lee, Physicochemical characteristics and in vitro toxicity/anti-SARS-CoV-2 activity of favipiravir solid lipid nanoparticles (SLNs), Pharmaceuticals [Internet] 14 (10) (2021 Oct 19) 1059. Available from: https://www.mdpi.com/1424-8247/14/10/1059.

[37] B. Lu, X. Lv, Y. Le, Chitosan-modified PLGA nanoparticles for control-released drug delivery, Polymers (Basel) [Internet] 11 (2) (2019 Feb 12) 304. Available from: https://www.mdpi.com/2073-4360/11/2/304.

[38] S. Dawre, P.V. Devarajan, A. Samad, Enhanced antibacterial activity of doxycycline and rifampicin combination loaded in nanoparticles against intracellular Brucella abortus, Curr. Drug. Deliv. [Internet] 19 (1) (2022 Jan) 104–116. Available from: https://www.eurekaselect.com/193997/article.

[39] S.K. Singh, P. Dadhania, P.R. Vuddanda, A. Jain, S. Velaga, S. Singh, Intranasal delivery of asenapine loaded nanostructured lipid carriers: formulation, characterization, pharmacokinetic and behavioural assessment, RSC Adv. [Internet 6 (3) (2016) 2032, 45. Available from: http://xlink.rsc.org/?DOI=C5RA19793G.

[40] R. Bellotti, G.B. Picotto, L. Ribotta, AFM measurements and tip characterization of nanoparticles with different shapes, Nanomanufacturing Metrol 5 (2) (2022) 127–138.

[41] P. Mura, N. Mennini, C. Nativi, B. Richichi, In situ mucoadhesive-thermosensitive liposomal gel as a novel vehicle for nasal extended delivery of opiorphin, Eur. J Pharm. Biopharm. [Internet] 122 (2018 Jan) 54–61. Available from: https://linighub.elsevier.com/retrieve/pii/S0939641117307026.

[42] S. Dawre, S. Pathak, S. Sharma, P.V. Devarajan, Enhanced antimalalarial activity of a prolonged release in situ gel of arteether–lumefantrine in a murine model, Eur. J. Pharm. Biopharm. [Internet 123 (2018 Feb) 95–107. Available from: https://linkinghub.elsevier.com/retrieve/pii/S0939641117306215.

[43] S.-H.S. Leung, J.R. Robinson, Polymer structure features contributing to mucoadhesion. II, J. Control Release [Internet] 12 (3) (1990 May) 187–194. Available from: https://linkinghub.elsevier.com/retrieve/pii/016836599090099F.

[44] D.-H. Kim, T.N. Nguyen, Y.-M. Han, P. Tran, J. Rho, J.-Y. Lee, et al., Local drug delivery using poly(lactic-co-glycolic acid) nanoparticles in thermosensitive gels for inner ear disease treatment, 77, Drug Deliv. [Internet]. 28 (1) (2021 Jan 1) 2268. Available from: https://www.tandfonline.com/doi/full/10.1080/10717544.2021.1992041.

[45] D.-H. Kim, D.C. Martin, Sustained release of dexamethasone from hydrophilic matrices using PLGA nanoparticles for neural drug delivery, Biomaterials [Internet] 27 (15) (2006 May) 3031–3037. Available from: https://linkinghub.elsevier.com/retrieve/pii/S0142961206000044.

[46] S. Dawre, S. Waghela, G. Saraogi, Statistically designed vitamin D3 Encapsulated PLGA microspheres dispersed in thermoresponsive in-situ gel for nasal delivery, J. Drug Deliv. Sci. Technol. [Internet] 75 (2022 Sep), 103688. Available from: https://linkinghub.elsevier.com/retrieve/pii/S1773224722005998.

[47] S. Bohrey, V. Chourasiya, A. Pandey, Polymeric nanoparticles containing diazepam: preparation, optimization, characterization, in-vitro drug release and release kinetic study, Nano. Converg. [Internet] 3 (1) (2016 Dec 1) 3. Available from: http://www.nanoconvergencejournal.com/content/3/1/3.

[48] S.A. Jain, D.S. Chauk, H.S. Mahajan, A.R. Tekade, S.G. Gattani, Formulation and evaluation of nasal mucoadhesive microspheres of Sumatriptan succinate, J. Microencapsul. [Internet 26 (8) (2009 Dec 5) 711–721. Available from: http://www.tandfonline.com/doi/full/10.3109/02652040802685241.

[49] S. Pund, G. Rasve, G. Borade, Ex vivo permeation characteristics of venlafaxine through sheep nasal mucosa, Eur. J. Pharm. Sci [Internet] 48 (1–2) (2013 Jan) 195–201. Available from: https://linkinghub.elsevier.com/retrieve/pii/S0928098712004320.

[50] S.S. Deshkar, M.S. Jadhav, S.V. Shirolkar, Development of carbamazepine nanostructured lipid carrier loaded thermosensitive gel for intranasal delivery, Adv. Pharm. Bull [Internet] 11 (1) (2020 Nov 7) 150–162. Available from: https://apb.tbzmed.ac.ir/Article/apb-28382.